Environ Geol (2005) 48: 920–930
DOI 10.1007/s00254-005-0030-2

ORIGINAL ARTICLE

Marijke Huysmans
Alain Dassargues

Stochastic analysis of the effect of heterogeneity and fractures on radionuclide transport in a low-permeability clay layer

Received: 05 June 2005
Accepted: 17 June 2005
Published online: 27 July 2005

M. Huysmans (✉) · A. Dassargues
KULeuven,
Department of Geology-Geography,
Hydrogeology and Engineering Geology Group,
Redingenstraat 16, 3000 Leuven, Belgium
E-mail: marijke.huysmans@geo.kuleuven.ac.be
Tel.: +32-16-326449
Fax: +32-16-326401

A. Dassargues
Hydrogeology and Environmental Geology, Department of Georesources, Geotechnologies and Building Materials (GEOMAC),
University of Liège,
B52/3, Liège, Belgium

Abstract Deep low-permeability clay layers are considered as safe environments for disposal of high-level radioactive waste. In Belgium, the Boom Clay is a candidate host rock for deep geological disposal. In this study, we analyze the effects of fractures and spatially variable hydraulic conductivity on radionuclide migration through the clay. Fracture geometry and properties are simulated with Monte Carlo simulation. The heterogeneity of hydraulic conductivity is simulated by direct sequential co-simulation using measurements of hydraulic conductivity and four types of secondary variables. The hydraulic conductivity and fracture simulations are used as input for a transport model. Radionuclide fluxes computed with this heterogeneous model are compared with fluxes obtained with a homogeneous model. The output fluxes of the heterogeneous model differ at most 8% from the homogeneous model. The main safety function of the Boom Clay is thus not affected by the fractures and the spatial variability of hydraulic conductivity.

Keywords Geostatistics · Waste disposal · Radionuclide transport · Fractures · Heterogeneous media

Introduction

Safe disposal of nuclear waste is an important environmental challenge. Several countries are investigating deep geological disposal as a long-term solution for high-level waste. In Belgium, France, Germany, Japan, Spain and Switzerland, clay layers are being considered as potential host formation (Landais 2004). In Belgium, the Boom Clay is a candidate host rock. This is a plastic clay of tertiary (Rupelian) age.

As part of the performance assessment of a disposal concept, the fate of radionuclides released from the potential repository is calculated. Radionuclide migration from the vitrified waste through the Boom Clay into the surrounding aquifers was examined in previous studies, which assumed that the clay layer was homogeneous (Mallants et al. 2001). These calculations showed that the magnitude of the fluxes released into the surrounding aquifers was strongly limited by the Boom Clay, so that the dose rates were a hundred times lower than the internationally recommended dose limit.

The Boom Clay is, however, like most natural deposits, not completely homogeneous. It contains alternating subhorizontal layers of silt and clay with an average thickness of 0.5 m and a large lateral continuity (Vandenberghe et al. 1997). The hydraulic conductivity of these layers varies between 10^{-12} and 10^{-10} m/s (Wemaere et al. 2002). Furthermore, the clay also exhibits excavation-induced fractures around the excavated galleries and tunnels (Dehandschutter et al. 2002).

Several studies have recognized that fractures and heterogeneity of hydraulic conductivity can have a significant effect on solute transport (e.g., Andersson et al. 2004; Xu et al. 2001; Pohlmann et al. 2000; Harrison et al. 1992; Rudolph et al. 1991). In this study, the effects of fractures and spatially variable hydraulic conductivity on radionuclide mass migration through the Boom Clay are examined. A large number of equally probable random realizations of the clay layer are generated using all available hard and soft data. These fields are used as input for a transport model that calculates transport by advection, diffusion, dispersion, adsorption and decay through the heterogeneous and fractured medium. Radionuclide fluxes at the clay-aquifer interfaces are calculated, taking the excavation-induced fractures and the heterogeneity of hydraulic conductivity into account. Radionuclide fluxes computed with this heterogeneous hydrogeological model are compared with fluxes obtained from a homogeneous model.

Method

Study site

The research activities of the Belgian nuclear repository program, conducted by ONDRAF/NIRAS (Belgian agency for radioactive waste and enriched fissile materials), are concentrated at SCK-CEN (Belgian Nuclear Research Centre) located in the nuclear zone of Mol-Dessel (province of Antwerp). An underground experimental facility (HADES-URF) was built in the Boom Clay at a depth of 223 m. In this area, the Boom Clay has a thickness of about 100 m and is overlain by 180 m of water-bearing sand formations (Fig. 1).

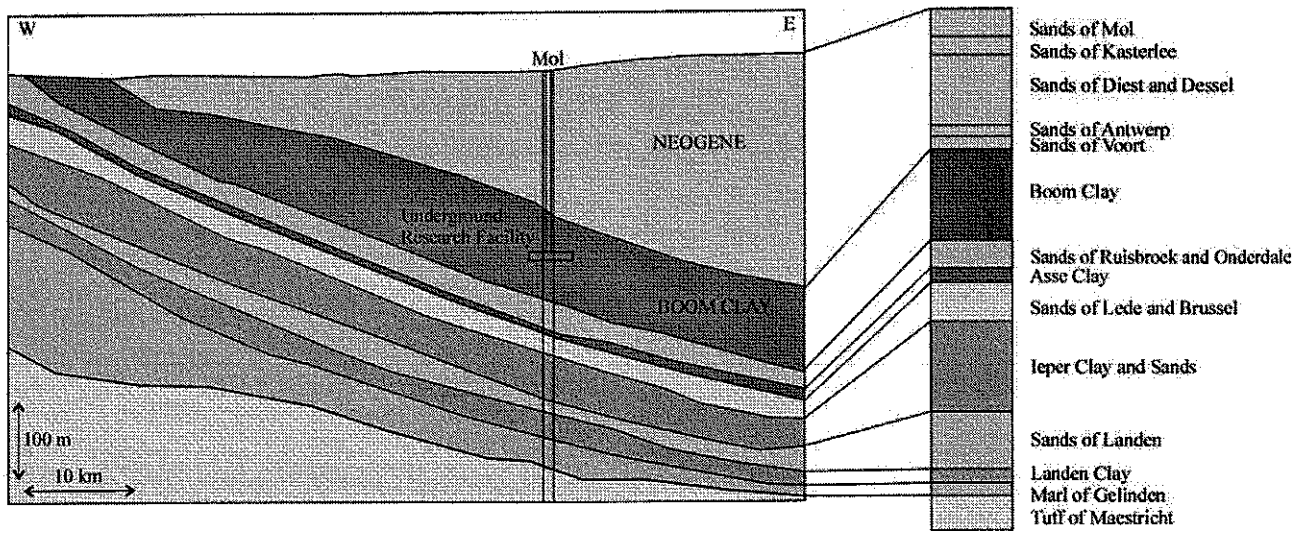

Fig. 1 Schematic view of the Boom Clay and the location of underground research facility (modified from Mallants et al. 2001)

Data analysis

To analyze and simulate the heterogeneous hydraulic conductivity of the Boom Clay, hydraulic conductivity measurements were collected. These are laboratory measurements carried out on centimeter scale samples of the cores from the Mol-1 borehole (Wemaere et al. 2002). Because of the scarcity of measurements of this primary variable of interest, measurements of secondary variables were also collected. Secondary variables are usually spatially cross-correlated with the primary variable and thus contain useful information about the primary variable. This cross-correlation between variables can be exploited to improve the estimates of the primary variable (Isaaks and Srivastava 1989). The resulting data set comprises 52 hydraulic conductivity values, a gamma ray log, an electrical resistivity log, 71 grain-size measurements and a detailed description of the lithology variation, all measured in the Mol-1 borehole (Fig. 2).

The value of incorporating the secondary information in the stochastic simulation of hydraulic conductivity was investigated by analyzing correlations between primary and secondary variables (Table 1). Electrical resistivity and hydraulic conductivity have a correlation coefficient of 0.73. The gamma ray, on the other hand, shows a negative and smaller correlation with hydraulic conductivity ($R=-0.65$). This relatively lower correlation is probably caused by the presence of organic matter and glauconite in the Boom Clay, both of which affect the gamma ray measurements. The correlation coefficient between d_{40} (i.e., the grain size for which 40% of the total sample has a smaller grain size) and hydraulic conductivity is 0.95. The lithostratigraphic

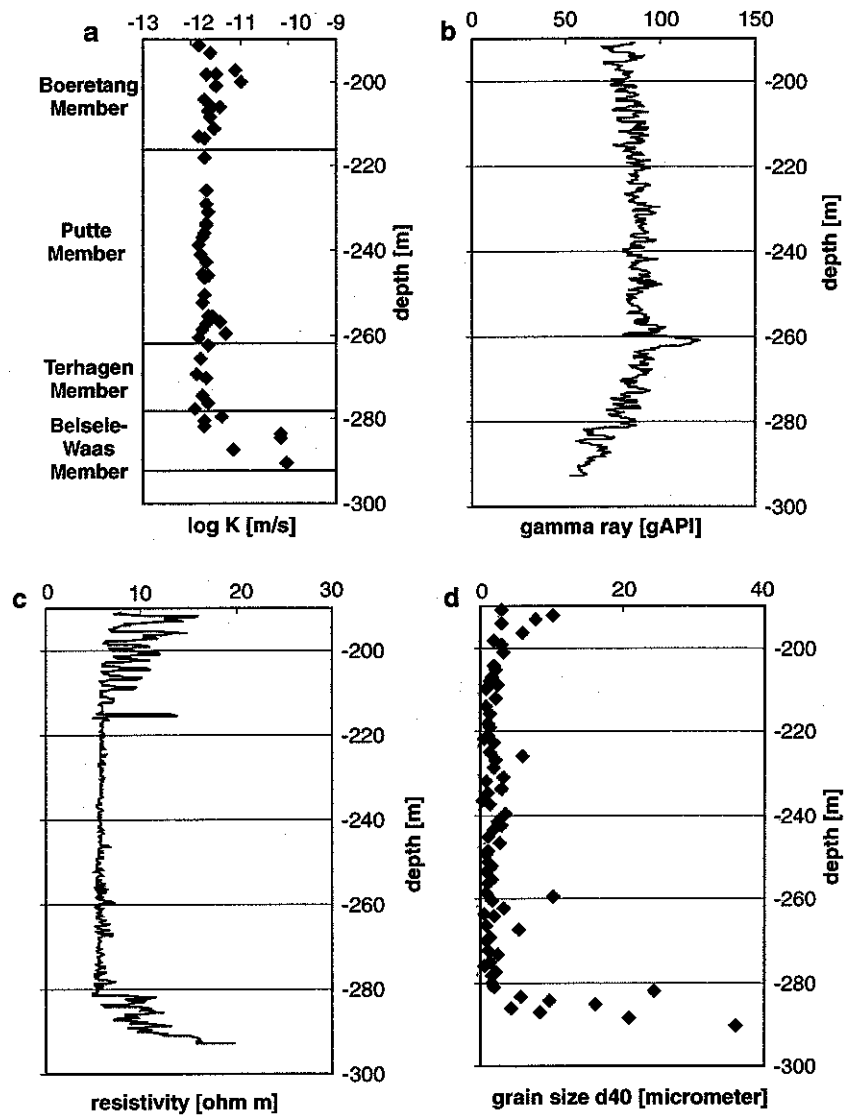

Fig. 2 **a** Hydraulic conductivity, **b** gamma ray, **c** resistivity and **d** grain size d_{40} of the Boom Clay in the Mol-1 borehole

column, determined on the basis of a Formation Micro Imager (FMI) log (Mertens and Wouters 2003), also shows a relationship with hydraulic conductivity: the mean log hydraulic conductivity of the clay layers (−11.7) is smaller than the mean log hydraulic conductivity of the silt layers (−11.3). All secondary measurements are thus well correlated with hydraulic conductivity and were therefore incorporated in the simulation of hydraulic conductivity.

In a previous work (Vandenberghe et al. 1997), the Boom Clay was divided into three zones. This subdivision was confirmed by statistical analysis. The deepest zone (Belsele-Waas Member: 278–292.4 m) shows a large variability of hydraulic conductivity and secondary variables, the middle zone (Putte and Terhagen Member: 216–278 m) shows a small variability and the upper zone (Boeretang Member: 190.4–216 m) shows an intermediate variability (Fig. 2). Variograms and cross-variograms of all the primary and secondary variables were calculated and modeled for the three separate zones. Table 2 shows the fitted log K variograms of the three zones of the Boom Clay. Examples of calculated and modeled variograms and cross-variograms are shown in Fig. 3.

Table 1 Correlation coefficients between hydraulic conductivity and secondary parameters

Secondary parameter	Correlation coefficient with hydraulic conductivity
Electrical resistivity	0.73
Gamma ray	−0.65
Grain size (d_{40})	0.95

Table 2 Fitted log K variograms of the three zones of the Boom Clay

	Model	Nugget	Range (m)	Sill
Boeretang member	Spherical	0.035	4.6	0.03
Rid Putte and Terhagen Member	Spherical	0.003	4.8	0.0056
Belsele-Waas	Spherical	0.23	5.5	0.38

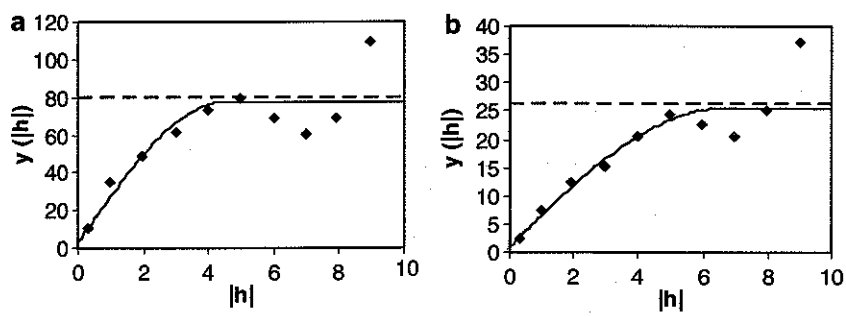

Fig. 3 Experimental and fitted **a** variogram of gamma ray of the Belsele-Waas Member in the vertical direction and **b** cross-variogram of gamma ray and resistivity in the Belsele-Waas Member in the vertical direction

Stochastic sequential simulation of hydraulic conductivity

The real spatial distribution of hydraulic conductivity of the Boom Clay is not completely known. Therefore, a large number of equally probable random realizations of the clay layer are generated. The realizations honor the measured data and the global statistics of hydraulic conductivity. The Boom Clay shows a lateral continuity that exceeds the extent of the local scale model (Wouters and Vandenberghe 1994). Therefore, it is assumed that the properties of the Boom Clay do not vary in the horizontal direction and 1D vertical realizations of hydraulic conductivity were generated.

The simulation algorithm is iterative and contains the following steps:

1. The location to be simulated is randomly chosen along the vertical axis. The spacing between the locations to be simulated is 0.2 m, which corresponds to the scale of the measurements.
2. The simple co-kriging estimate and variance are calculated using the original primary and secondary data and all previously simulated values using COKB3D (Deutsch and Journel 1998).
3. The shape of the local hydraulic conductivity distribution in each location is determined in such a way that the original histogram of hydraulic conductivity is reproduced by the simulation. This is achieved by the following approach (Oz et al. 2003). Before the start of the simulation, a look-up table is constructed by generating non-standard Gaussian distributions by choosing regularly spaced mean values (approximately from −3.5 to 3.5) and variance values (approximately from 0 to 2). The distribution of uncertainty in the data space can then be determined from back transformations of these nonstandard univariate Gaussian distributions by back transformation of L regularly spaced quantiles, $p^l, l = 1, \ldots, L$:

$$K^l = F_K^{-1}\left[G\left(G^{-1}(p^l)\sigma_y + y^*\right)\right], \quad l = 1, ..., L$$

where F_K (K) is the cumulative distribution function from the original K variable, $G(y)$ is the standard normal cumulative distribution function, y^* and σ_y are the mean and standard deviation of the nonstandard Gaussian distribution and the $p^l, l = 1, \ldots, L$ are uniformly distributed values between 0 and 1. From this look-up table the closest K-conditional distribution is retrieved by searching for the one with the closest mean and variance to the co-kriging values (Oz et al. 2003).
4. A value is drawn from the K-conditional distribution by Monte Carlo simulation and assigned to the location to be simulated. This approach creates realizations that reproduce (1) the local point and block data in the original data units, (2) the mean, variance and variogram of the variable and (3) the histogram of the variable (Oz et al. 2003).

For this study, a total of ten realizations of the vertical hydraulic conductivity of the Boom Clay are generated using this approach. Figure 4 shows one realization.

Stochastic simulation of fractures

Around the galleries and tunnels in the Boom Clay, excavation-induced fractures are observed. Fracture analysis carried out during recent tunnel excavation in the Boom Clay (Dehandschutter et al. 2002; Dehandschutter 2002; Mertens et al. 2004) revealed that the most dominant discontinuities are part of a twofold conjugated fault set (Fig. 5). They are approximately parallel planes with an average spacing of around 70 cm,

an extent of approximately 2 m, a strike approximately perpendicular to the tunnel axis and a dip between 30 and 70°. The excavation-induced fractures around the future disposal galleries in the Boom Clay will probably have similar properties to these observed fractures. Their properties (i.e. extent, aperture, spacing, dip and strike) are therefore simulated using Monte Carlo simulation with input probability distributions of the fracture properties derived from the measurements. Fractures in argillaceous are often cited to have the capacity to self-heal or become, with the passage of time, less conductive to groundwater (Horseman, 2001). In this study, it is conservatively assumed that no self-healing occurs.

Examination of a mounting chamber excavated in the Boom Clay revealed that the rock mass seemed to be damaged up to approximately 2 m from the excavation with a lot of small-scale disturbances. The observed fractures were open and pyrite oxidation occurred on the surfaces till 2 m of depth (Mertens et al. 2004). Therefore, the average extent of the simulated fractures was set to 2 m. To account for uncertainty in clay properties, tunnel design or excavation techniques, some variation of the extent of the fractured zone was allowed. The extent of the fractures was therefore simulated as a random number between 1 and 3 m.

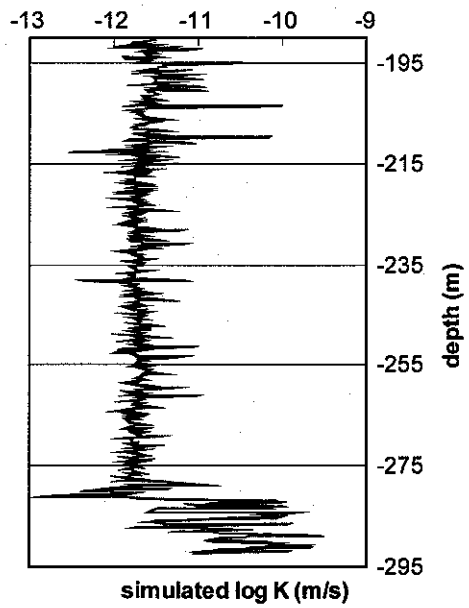

Fig. 4 Simulation of vertical hydraulic conductivity of the Boom Clay. The large variability in the deepest zone (Belsele-Waas Member) reflects the higher sill of the variogram in that zone

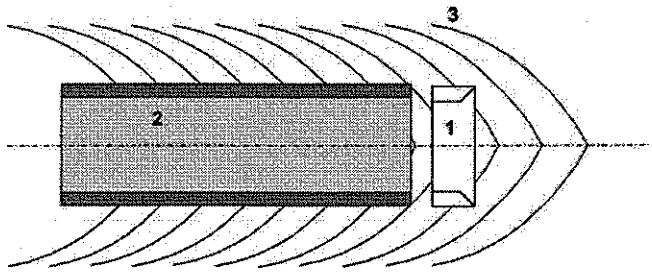

Fig. 5 Schematical representation of a vertical cross-section through the Connecting Gallery showing the typical symmetrical form of the encountered shear planes (*1* tunneling maching; *2* supported tunnel; *3* induced shear planes)

Fracture apertures in the Boom Clay were examined using microtomography and scanning electron microscopy (Dehandschutter et al. 2004). Values of tens of micrometers were measured. The aperture could be as large as 1 mm at the tunnel walls and decreased rapidly as the distance to the excavation increased (B. Dehandschutter, personal communication). Therefore, fracture aperture was simulated as a random number between 0 and 50μm.

Faulting is very intense over most part of the excavation zone. The distance between subsequent fractures is generally less than 1 m. The average spacing is about 70 cm (Mertens et al. 2004). The fracture spacing was drawn from a distribution reflecting these observations, i.e. a normal distribution with a mean of 0.70 m and a standard deviation of 0.12 m.

Fracture dip angle varies between 30 and 80° (Dehandschutter et al. 2002). Eighty-two fracture dip measurements of shear faults were carried out (Dehandschutter 2002). The average fracture dip was 53° and the standard deviation was 11°. The fracture dip was therefore drawn from a normal distribution with a mean of 53° and a standard deviation of 11°.

Examination of the strike of discontinuities surrounding boreholes and larger excavations in the Boom Clay revealed that the strike of most discontinuities was perpendicular to the borehole or gallery axis (Dehandschutter 2002). The orientation of the fractures was fairly constant and all fractures were therefore assumed to have a strike perpendicular to the gallery axis.

For this study, a total of ten realizations of fracture geometry and properties are simulated by independent sampling from the proposed marginal distributions of fracture extent, aperture, spacing, dip and strike.

Hydrogeological model

A local 3D hydrogeological model of the Boom Clay, including the simulations of matrix hydraulic conductivity values and fractures, was constructed. The model width in the *x*-direction is 20 m, i.e., half the distance between the disposal galleries (Fig. 6). The model length in the *y*-direction is 15 m. This length was a compromise between including as many fractures as possible and keeping the computation time manageable. The model dimension in the *z*-direction is 102 m, i.e., the total thickness of the Boom Clay in the nuclear zone of Mol-

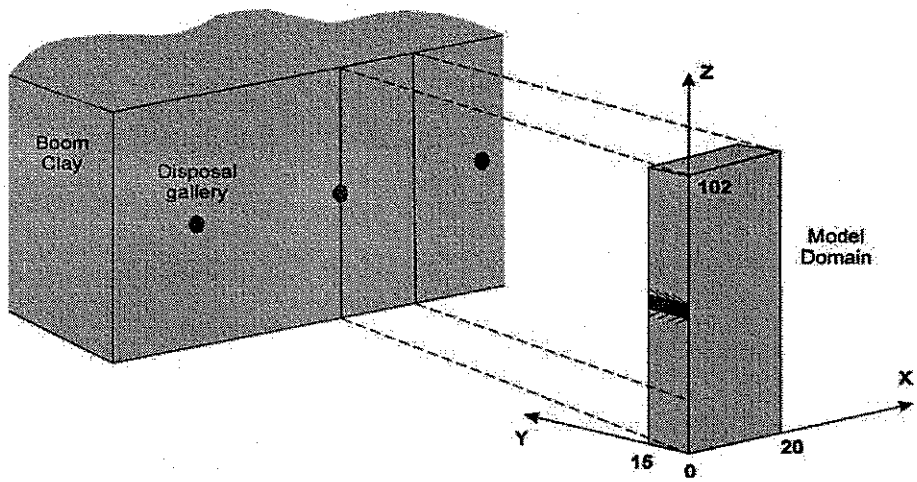

Fig. 6 Model domain of 3D local hydrogeological model

Dessel. The grid spacing is 1 m in the x-direction, approximately 0.17 m in the y-direction and varies between 0.2 and 1 m in the z-direction. This fine grid was necessary to include the high-resolution simulations of hydraulic conductivity and the geometry of the fractures. The boundary conditions for groundwater flow and transport are shown in Fig. 7. The vertical boundary conditions for groundwater flow are zero flux boundary conditions since the hydraulic gradient is vertical. The horizontal boundary conditions for groundwater flow are Dirichlet conditions. The specified head at the upper boundary is 2m higher than the specified head at the lower boundary since the downward vertical hydraulic gradient is approximately 0.02 in the 100 m thick Boom Clay (Wemaere and Marivoet 1995). The boundary conditions for transport at the upper and lower boundaries are zero concentration boundary conditions (Mallants et al. 1999) since the hydraulic conductivity contrast between the clay and the aquifer is so large that solutes reaching the boundaries are assumed to be flushed away by advection in the aquifer.

The transport model was calculated for three radionuclides: Se-79, I-129 and Tc-99. Previous calculations revealed that they were the most important in terms of dose rates from a potential high-level waste repository for vitrified waste (Mallants et al. 1999). The properties of these radionuclides are given in Table 3. The transport processes that were taken into account in the model are advection, dispersion, molecular diffusion, linear and reversible sorption and radioactive decay.

The source term models for the three radionuclides are as described by Mallants et al. 1999. The radionuclides are contained in borosilicate glass and as the glass corrodes, the radionuclides become available for dissolution into the groundwater. A constant glass dissolution rate of 3 μm year^{-1} was assumed. Since the initial radius of the cylindrical glass matrix would be 0.215 m, the glass matrix would be completely dissolved after approximately 70,000 years. The source term model is therefore a constant flux over a period of 70,000 years equal to the total radionuclide inventory divided by 70,000 years. If, however, this source term model re-

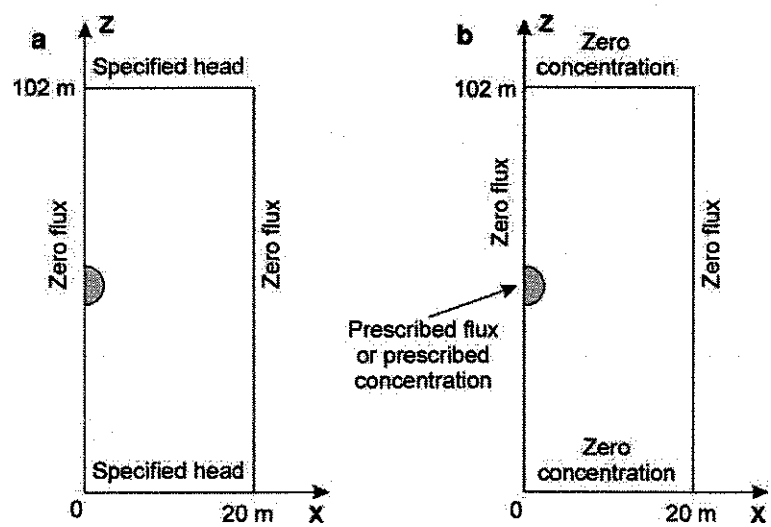

Fig. 7 Boundary conditions for **a** flow and **b** transport of 3D local hydrogeological model

Table 3 Properties of selected radionuclides (values are taken from Mallants et al. 1999)

	Se-79	I-129	Tc-99
Half-life (year)	6.50×10^{4}	1.57×10^{7}	2.13×10^{5}
Decay constant ($year^{-1}$)	1.07×10^{-5}	4.41×10^{-8}	3.25×10^{-6}
Solubility limit (mol l^{-1})	5.5×10^{-8}	–	3×10^{-8}
Diffusion coefficient ($m^2\ s^{-1}$)	2×10^{-10}	2×10^{-10}	2×10^{-10}
Diffusion-accessible porosity	0.13	0.12	0.30
Retardation factor	1	1	1

sulted in calculated concentrations higher than the solubility limit, the source term model was replaced by a constant concentration model. A constant concentration equal to the solubility limit was then prescribed until exhaustion of the source.

This local 3D hydrogeological model was run with FRAC3DVS, a simulator for 3D groundwater flow and solute transport in porous, discretely fractured porous or dual-porosity formations (Therrien et al. 1996, 2003). The fractures were modeled as discrete planes with a saturated hydraulic conductivity of (Bear 1972):

$$K_f = \frac{\rho g(2b)^2}{12\mu}$$

where ρ is the fluid density (kg/m^3), g the acceleration due to gravity (m/s^2), $2b$ the fracture aperture (m) and μ the fluid viscosity (kg/ms). Since the fracture aperture in this study was simulated as a random number between 0 and 50 μm, K_f lies between 0 and 6.25×10^{-3} m/s and has an average value of approximately 2×10^{-3} m/s.

This local 3D hydrogeological model was run for ten different random combinations of simulations of hydraulic conductivity and simulations of fractures. The results of this model were compared with the results of a homogeneous model.

Results

Figure 8 shows the computed total Se-79 fluxes through the lower and upper clay-aquifer interfaces for the ten different simulations. The Se-79 fluxes through the clay-

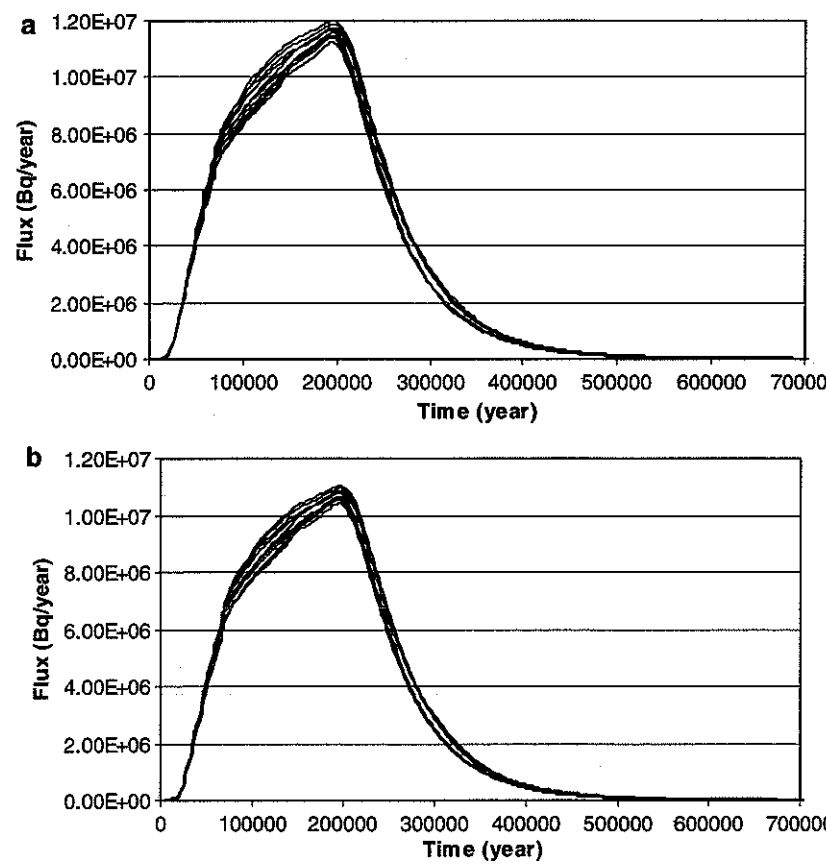

Fig. 8 Total calculated Se-79 flux (Bq/year) (**a**) through the lower clay-aquifer interface and (**b**) through the upper clay-aquifer interface

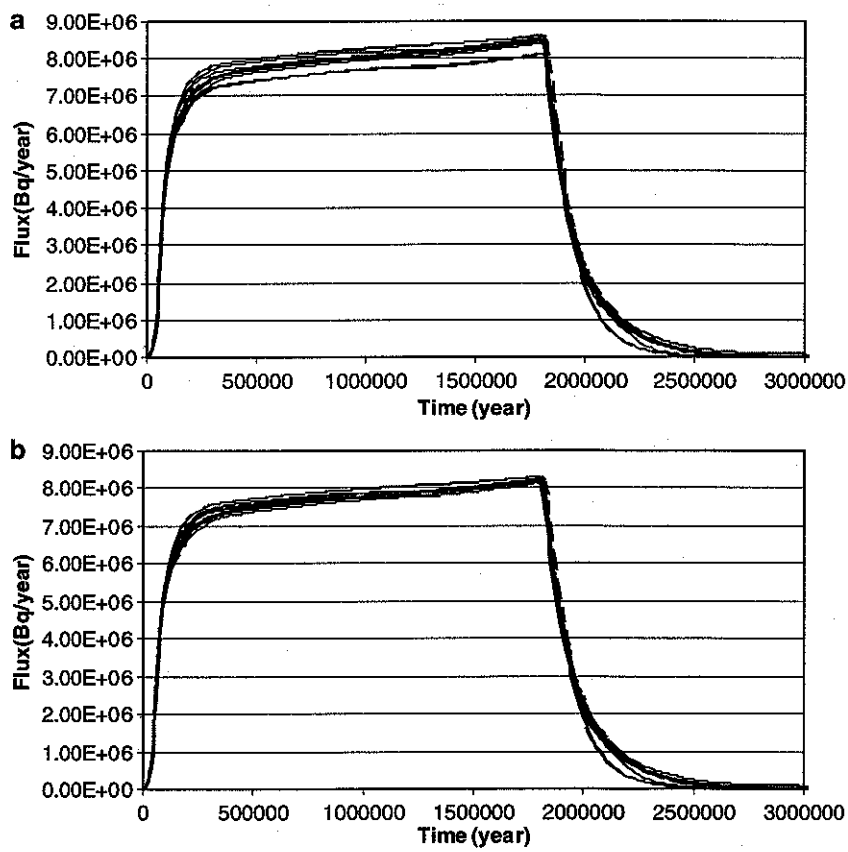

Fig. 9 Total calculated Tc-99 flux (Bq/year) **a** through the lower clay-aquifer interface and **b** through the upper clay-aquifer interface

aquifer interfaces gradually increase until they reach a maximum after approximately 200,000 years and decrease slowly afterwards due to exhaustion of the source. The difference between the radionuclide flux through the lower and upper boundary is caused by downward advection. The difference between the fluxes of the ten different simulations is the largest in the time period from 100,000 to 200,000 years. The total amount of Se-79 leaving the clay was calculated as flux integrated over time for each simulation. The total Se-79 mass leaving the clay vary between 2.200×10^{12} Bq and 2.438×10^{12} Bq through the lower clay-aquifer interface and between 2.045×10^{12} Bq and 2.252×10^{12} Bq through the upper clay-aquifer interface.

Figure 9 shows the computed total Tc-99 fluxes through the lower and upper clay-aquifer interfaces for ten different simulations. The Tc-99 fluxes through the clay-aquifer interfaces increase relatively fast the first 200,000 years. From 200,000 to 1,750,000 years, the fluxes increase more gradually. The fluxes decrease afterwards due to exhaustion of the source. The difference between the fluxes of the ten different simulations is the largest in the time period from 200,000 to 1,750,000 years. The total Tc-99 mass leaving the clay vary between 1.423×10^{13} Bq and 1.541×10^{13} Bq through the lower clay-aquifer interface and between 1.443×10^{13} and 1.489×10^{13} Bq through the upper clay-aquifer interface.

The calculated I-129 fluxes through the lower and upper clay-aquifer interfaces for ten simulations are shown in Fig. 10. The differences between the fluxes of the different simulations are rather small. The fluxes through the clay-aquifer interfaces increase until they reach a maximum after approximately 120,000 years and decrease slowly afterwards. The total I-129 mass leaving the clay vary between 2.957×10^{11} and 3.006×10^{11} Bq through the lower clay-aquifer interface and between 2.714×10^{11} and 2.757×10^{11} Bq through the upper clay-aquifer interface.

In Fig. 11, a comparison is made between the radionuclide masses calculated with the heterogeneous simulations and the homogeneous model. The figure shows boxplots of the difference in percentage of total radionuclide mass between the heterogeneous and the homogeneous models. Compared to the homogeneous model, the radionuclide mass flowing through the lower clay-aquifer is between 8% smaller and 4% larger in the heterogeneous model. The radionuclide mass flowing through the upper clay-aquifer is between 4% smaller and 6% larger.

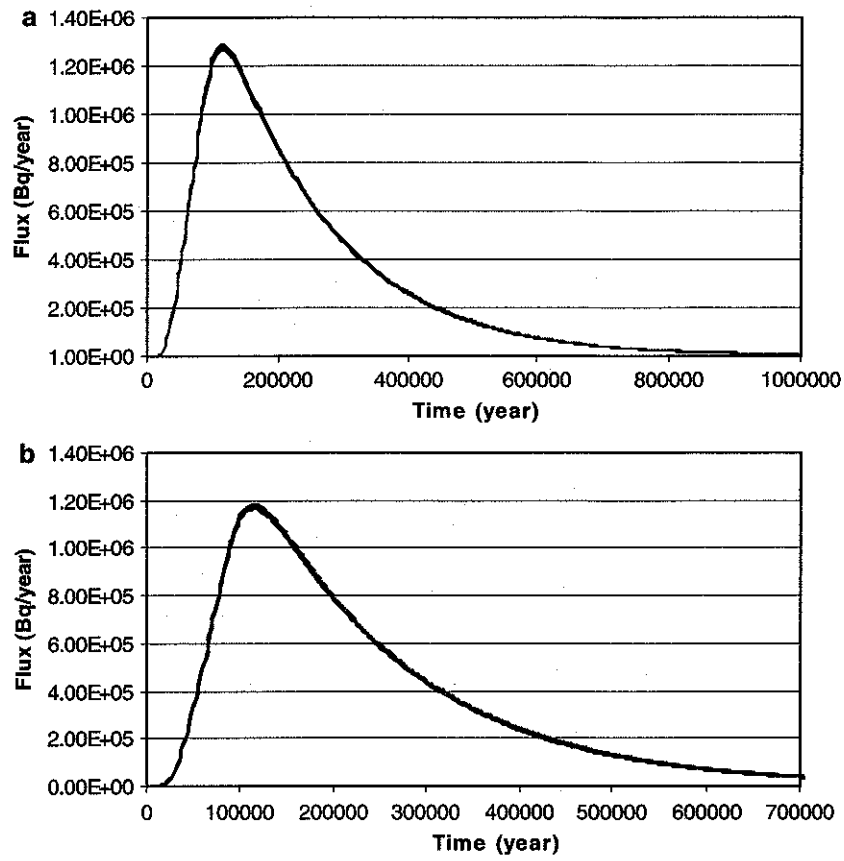

Fig. 10 Total calculated I-129 flux (Bq/year) **a** through the lower clay-aquifer interface and **b** through the upper clay-aquifer interface

Discussion

The range of the output radionuclide masses of the ten different simulations is limited. The difference between the largest and the smallest calculated radionuclide masses leaving the clay is about 10%. The difference between the fluxes of the heterogeneous simulations and the homogeneous model is also rather small. The output fluxes of the heterogeneous model differ at most 8% from the fluxes of the homogeneous model.

This result is important for the evaluation of the suitability of the Boom Clay as a host rock for vitrified nuclear waste storage. The total mass fluxes leaving the clay, taking excavation-induced fractures and high-conductivity sublayers into account, are not very different from the mass fluxes calculated by a simple homogeneous model. Therefore, changes in the hetero-

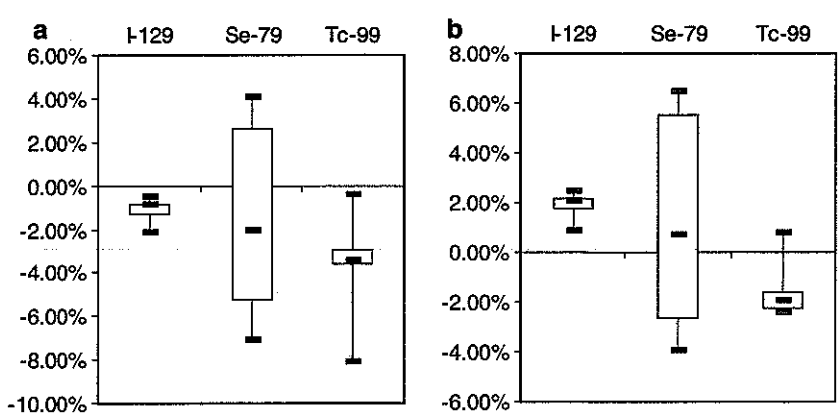

Fig. 11 Boxplots of difference in percentage of total radionuclide mass between heterogeneous and homogeneous models **a** through the lower clay-aquifer interface and **b** through the upper clay-aquifer interface

geneity of hydraulic conductivity do not change the output fluxes significantly and do not affect its main safety function. This again shows that the Boom Clay is a very robust barrier.

The small effect of hydraulic conductivity heterogeneity and of fractures is probably caused by the relatively small importance of transport by advection compared to transport by diffusion in low- permeability media. Diffusion is usually the dominating transport process in clay layers while the contribution of transport by advection is limited. Investigating the effect of the heterogeneity of the diffusion parameters is therefore the subject of further research.

It must also be noted that in this research only fractures around horizontal galleries are included. The fractured zone around the vertical shaft connecting the galleries with the surface is not modeled since the purpose of this study was to investigate the effect of geological heterogeneity and fractures on transport through the clay itself. The fractured zone around the vertical shaft may, however, possibly be a fast pathway for radionuclides to the surface and will also be the subject of further research.

Conclusions

In this study, the transport of radionuclides through a potential host formation for the disposal of vitrified nuclear waste was calculated, taking the geological heterogeneity and the excavation-induced fractures into account. The calculated fluxes through the clay boundaries into the surrounding aquifers were very similar for all the different simulations and were also very similar to the fluxes calculated with a homogeneous model. These results show that changes in the heterogeneity of hydraulic conductivity do not change the output fluxes significantly. The robust barrier function of the Boom Clay is thus confirmed by these results.

Acknowledgements The authors wish to acknowledge the Fund for Scientific Research—Flanders for providing a Research Assistant scholarship to the first author. We also wish to thank ONDRAF/NIRAS (Belgium agency for radioactive waste and enriched fissile materials) and SCK-CEN (Belgian Nuclear Research Centre) for providing the necessary data for this study. We also thank René Therrien and Rob McLaren for providing FRAC3DVS and for their assistance.

References

Andersson P, ByegÅrd J, Tullborg EL, Doe T, Hermanson J, Winberg A (2004) In situ tracer tests to determine retention properties of a block scale fracture network in granitic rock at the Äspö Hard Rock Laboratory, Sweden. J Contam Hydrol 70(3–4):271–297

Bear J (1972) Dynamics of fluids in porous media. American Elsevier, New York

Dehandschutter B (2002) Faulting and Fracturing during Connecting Gallery tunnelling at the URL at Mol (SCK-CEN). ONDRAF/NIRAS internal report, Brussel, Belgium

Dehandschutter B, Sintubin M, Vandenberghe N, Vandycke S, Gaviglio P, Wouters L (2002) Fracture analysis in the Boom Clay (URF, Mol, Belgium). Aardkundige Mededelingen 12:245–248

Dehandschutter B, Vandycke S, Sintubin M, Vandenberghe N, Gaviglio P, Sizun JP, Wouters L (2004) Microfabric of fractured Boom Clay at depth: a case study of brittle-ductile transitional clay behaviour. Appl Clay Sci 26(1–4):389–401

Deutsch CV, Journel AG (1998) GSLIB geostatistical software library and user's guide. Oxford University Press, New York

Harrison B, Sudicky EA, Cherry JA (1992) Numerical analysis of solute migration through fractured clayey deposits into underlying aquifers. Water Resource Res 28(2):515–526

Horseman ST (2001) Self-healing of fractures in argillaceous media from the geomechanical point of view. In: Self-healing topical session proceedings, 11th Clay Club meeting, Nancy, OCDE/NEA, Paris

Isaaks EH, Srivastava RM (1989) An introduction to applied geostatistics. Oxford University Press, New York

Landais P (2004) Clays in natural and engineered barriers for radioactive waste confinement. Appl Clay Sci 26(1–4):1

Mallants D, Sillen X, Marivoet J (1999) Geological disposal of conditioned high-level and long lived radioactive waste: consequence analysis of the disposal of vitrified high-level waste in the case of the normal evolution scenario. Ondraf/Niras report R-3383, Brussel, Belgium

Mallants D, Marivoet J, Sillen X (2001) Performance assessment of vitrified high-level waste in a clay layer. J Nucl Mater 298(1–2):125–135

Mertens J, Wouters L (2003) 3D Model of the Boom Clay around the HADES-URF. NIROND report 2003–02, Brussel, Belgium

Mertens J, Bastiaens W, Dehandschutter B (2004) Characterization of induced discontinuities in the Boom Clay around the underground excavations (URF, Mol, Belgium). Appl Clay Sci 26(1–4):413–428

Oz B, Deutsch CV, Tran TT, Xie Y (2003) DSSIM-HR: a FORTRAN 90 program for direct sequential simulation with histogram reproduction. Comput Geosci 29(1):39–51

Pohlmann K, Hassan A, Chapman J (2000) Description of hydrogeologic heterogeneity and evaluation of radionuclide transport at an underground nuclear test. J Contam Hydrol 44(3–4):353–386

Rudolph DL, Cherry JA, Farvolden RN (1991) Groundwater flow and solute transport in fractured lacustrine clay near Mexico City. Water Resource Res 27(9):2187–2201

Therrien R, Sudicky EA (1996) Three-dimensional analysis of variably-saturated flow and solute transport in discretely-fractured porous media. J Contam Hydrol 23 (1–2):1–44

Therrien R, Sudicky EA, McLaren RG (2003) FRAC3DVS: an efficient simulator for three-dimensional, saturated-unsaturated groundwater flow and density dependent, chain-decay solute transport in porous, discretely-fractured porous or dual-porosity formations, User's guide

Vandenberghe N, Van Echelpoel E, Laenen B, Lagrou D (1997) Cyclostratigraphy and climatic eustacy—example of the Rupelian stratotype. Comptes Rendus de l'Academie des Sciences. Earth Planet Sci 325:305–315

Wemaere I, Marivoet J (1995) Geological disposal of conditioned high-level and long lived radioactive waste: updated regional hydrogeological model for the Mol site (The north-eastern Belgium model). ONDRAF/NIRAS Report R-3060, Brussel, Belgium

Wemaere I, Marivoet J, Labat S, Beaufays R, Maes T (2002) Mol-1 borehole (April-May 1997): core manipulations and determination of hydraulic conductivities in the laboratory. ONDRAF/NIRAS Report R-3590, Brussel, Belgium

Wouters L, Vandenberghe N (1994) Geologie van de Kempen: een synthese. ONDRAF/NIRAS Report NIROND-94–11, Brussel, Belgium

Xu S, Worman A, Dverstorp B (2001) Heterogeneous matrix diffusion in crystalline rock—implications for geosphere retardation of migrating radionuclides. J Contam Hydrol 47 (2–4):365–378